

Showcasing research from the Institute of Chemistry at the National Autonomous University of Mexico

Acidity and basicity interplay in amide and imide self-association

We found that the differences in the self-association of imides and amides are determined by a balance between acidity (red lights) and basicity (blue lights) of the N-H and C=O groups, respectively. Our model, obtained by NMR experiments and quantum chemical calculations, represents an alternative explanation for the surprisingly stronger dimerisation of amides than that offered by the secondary interaction hypothesis. The artwork is due to Dr Víctor Duarte Alaniz (braquistos@gmail.com).

As featured in:



See Marcos Hernández-Rodríguez, Tomás Rocha-Rinza et al., *Chem. Sci.*, 2018, 9, 4402.



rsc.li/chemical-science

Registered charity number: 207890

Cite this: *Chem. Sci.*, 2018, 9, 4402

Acidity and basicity interplay in amide and imide self-association†

Wilmer E. Vallejo Narváez,[‡] Eddy I. Jiménez,[‡] Eduardo Romero-Montalvo,[‡] Arturo Sauza-de la Vega,[‡] Beatriz Quiroz-García, Marcos Hernández-Rodríguez^{‡*} and Tomás Rocha-Rinza^{‡*}

Amides dimerise more strongly than imides despite their lower acidity. Such an unexpected result has been rationalised in terms of the Jorgensen Secondary Interactions Hypothesis (JSIH) that involves the spectator (C=O_S) and H-bonded (C=O_{HB}) carbonyl groups in imides. Notwithstanding the considerable body of experimental and theoretical evidence supporting the JSIH, there are some computational studies which suggest that there might be other relevant intermolecular interactions than those considered in this model. We conjectured that the spectator carbonyl moieties could disrupt the resonance-assisted hydrogen bonds in imide dimers, but our results showed that this was not the case. Intrigued by this phenomenon, we studied the self-association of a set of amides and imides *via* ¹H-NMR, ¹H-DOSY experiments, DFT calculations, QTAIM topological analyses of the electron density and IQA partitions of the electronic energy. These analyses revealed that there are indeed repulsions of the type O_S··O_{HB} in accordance with the JSIH but our data also indicate that the C=O_S group has an overall attraction with the interacting molecule. Instead, we found correlations between self-association strength and simple Brønsted–Lowry acid/base properties, namely, N–H acidities and C=O basicities. The results in CDCl₃ and CCl₄ indicate that imides dimerise less strongly than structurally related amides because of the lower basicity of their carbonyl fragments, a frequently overlooked aspect in the study of H-bonding. Overall, the model proposed herein could provide important insights in diverse areas of supramolecular chemistry such as the study of multiple hydrogen-bonded adducts which involve amide or imide functional groups.

Received 3rd March 2018

Accepted 5th April 2018

DOI: 10.1039/c8sc01020j

rsc.li/chemical-science

Introduction

Hydrogen bonds (HBs) in amides and imides are ubiquitous directional forces in nature. HBs in these functional groups are responsible for the secondary interactions, along with other interactions of the tertiary and quaternary structures of proteins.^{1,2} Other molecules in which hydrogen bonding is relevant are nucleic acids. The recognition among nitrogenous bases such as uracil and thymine is crucial in the DNA, RNA and other related systems.³ Besides HBs, base stacking, steric and

electrostatic effects can be important in the stabilisation of nucleic acids.⁴ Additionally, the dimerisation of amides and imides is of interest in several fields such as supramolecular chemistry in which the self-recognition of these functional groups is relevant.^{5,6}

The formation of amide and imide dimers is frequently studied by NMR or IR spectroscopy to determine self-association constants in solution.^{7,8} Rebek and co-workers⁹ examined the intramolecular imide–imide and amide–amide association through NMR measurements. The corresponding results indicate that despite their lower acidity, amides exhibit stronger self-associations than imides. Electronic structure calculations made by Jorgensen and co-workers are consistent with these unexpected experimental observations.¹⁰ We consider herein a rationalisation of the surprising stronger self-association of amides as compared with imides based on three different criteria.

(i) Repulsions involving the spectator carbonyls of imides

The Jorgensen Secondary Interactions Hypothesis (JSIH),¹¹ is usually invoked to explain the larger K_{dimer} of amides as compared to imides in spite of their lower acidic character.^{9,10} The JSIH considers that amides and imides have a similar kind

Institute of Chemistry, National Autonomous University of Mexico, Ciudad Universitaria, Circuito Exterior, Del. Coyoacán, Mexico City, 04510, Mexico. E-mail: marcoshr@unam.mx; tomasrocharinza@gmail.com

† Electronic supplementary information (ESI) available: Experimental and computational details. Protocol for the recording of ¹H-DOSY and ¹H-NMR titrations (A1, A2, A4–A7, I1–I5 and I8). Correlations of the computed acidity and basicity with experimental data. Molecular graphs of the monomers and dimers of amides and imides computed with SMD-M06-2x/6-311++G(2d,2p) electron densities. Characterisation of selected HBs in terms of the topological properties of $\rho(\mathbf{r})$ such as delocalisation index and the Interacting Quantum Atoms energy partition. XYZ coordinates and electronic energies of all species addressed in the paper. See DOI: 10.1039/c8sc01020j

‡ Present address: Department of Chemistry, University of British Columbia, Okanagan, 3247 University Way, Kelowna, British Columbia, Canada V1V 1V7.



deuterated solvents such as chloroform-*d*, acetonitrile-*d*₃ and DMSO-*d*₆, and also considered the reported value in CCl₄ in order to select the most suitable solvent for this research. Another feature of 2-pyrrolidone which makes it particularly suitable for this purpose is the fact that it is liquid at room temperature and thereby its self-association is easier to study in deuterated solvents which cover a broad range of polarity. As expected, K_{dimer} diminishes with the polarity of the medium (Table 1), to the point that it is very complicated to reliably determine the self-association constant of **A1** in solvents as polar as DMSO. Additionally, common imides are usually found as crystalline solids and therefore they are rather insoluble in apolar environments. Hence, we decided to carry out the measurements of K_{dimer} in chloroform-*d* due to its optimal compromise between the solubility of the investigated systems and the possibility to accurately determine their self-association constants. The attainment of this compromise prevented the analysis of a larger collection of amides and imides than that considered in this paper.

Next, we employed ¹H-DOSY experiments to evaluate if imide and amide dimers are indeed the predominant supramolecular aggregates in CDCl₃. This circumstance is particularly relevant in the case of imides for which it has been suggested that larger clusters might be formed in solution²¹ while polymeric structures can occur in the solid state.²² More specifically, we used this technique to determine the hydrodynamic radii (r_{H}) of the studied amide and imide dimers as reported in Table 2 (the structures of the referred compounds are displayed in Table 3). In addition, we also computed the theoretical hydrodynamic radii from electronic structure calculations (r_{calc}). As expected, structurally similar compounds have close values for r_{H} and r_{calc} , e.g., the radii of amides **A1**, **A2** and imide **I4** are alike because all of them are unsubstituted five-membered rings. **A4**, **A5** and **I1** are likewise six-membered heterocycles with closely related structures as reflected in their values of r_{calc} and r_{H} . Nevertheless, the cyclic chains in the uracil derivatives **I5** and **I8** and the benzo-derivatives **A6**, **A7** and **I3** introduce discrepancies between r_{H} and r_{calc} . This condition occurs because the spherical particle model employed in the estimation of r_{H} does not represent the oblate spheroid character of these dimers. Despite these differences, the experimental r_{H} values are always smaller than the computed r_{calc} data (apart from **I8** for which r_{calc} and r_{H} are similar). These results indicate that the investigated amides and imides do not form trimers or larger clusters to an appreciable extent.

Once we chose a suitable solvent and verified that the dimeric species are indeed predominantly formed in solution, we consider now the compounds shown in Table 3. This

Table 1 K_{dimer} of 2-pyrrolidone in different solvents at 25 °C

Solvent	K_{dimer} (M ⁻¹)
Carbon tetrachloride	145.0 (ref. 10)
Chloroform- <i>d</i>	2.7 ^a
Acetonitrile- <i>d</i> ₃	0.3 ^a
DMSO- <i>d</i> ₆	<0.1

^a Error values below 1% (see Fig. S1 in the ESI).

Table 2 Hydrodynamic radii estimated from ¹H-DOSY experiments (r_{H}) and computed with the SMD-M06-2x/6-311G++(2d,2p) approximation (r_{calc}). The values are reported in angstroms

Compound	r_{H} ^a	r_{calc}
A1	3.49	4.04
A2	3.57	3.96
A4	4.16	4.29
A5	4.01	4.33
A6	3.77	5.30
A7	4.11	5.33
I1	4.33	4.46
I2	5.52	5.81
I3	5.04	6.18
I4	3.39	4.03
I5	5.12	6.30
I8	10.58	9.67

^a TMS as an internal standard reference.²³

collection of systems contains a good variety of structures and even some previously reported derivatives of nitrogenous bases found in RNA.³ In agreement with previous studies,⁹ the self-association of amides is stronger than that of imides for molecules with the same ring size and unsaturation patterns, e.g., **A5** vs. **I1**, **A1** vs. **I2**, **A6** vs. **I3** and **A4** vs. **I6–I13**. These results point out that an increase in acidity does not necessarily lead to a stronger self-association. For example, the decreasing orders of acidity of the structurally related imides (**I7–I11**) are **I7** > **I11** > **I8** > **I9**, while those of dimerisation are backwards. We found, however, also exceptions to this behaviour, for instance **A5** vs. **A4** and **I5** vs. **I8** in which acidity and self-association increase in the same direction. Based on the above experimental results, now we proceed to examine the three considered hypotheses concerning the comparison of the self-association between amides and imides.

(i) Repulsions involving the spectator carbonyls of imides.

We test here the hypothesis that repulsions involving the spectator carbonyl groups are responsible for the smaller degree of dimerisation of imides as compared with that of amides. For this purpose, we used electron density topology analyses in accordance with the QTAIM theory and the IQA approach. The results shown in Fig. 2 indicate that the intermolecular interactions present in the amide **A5** and the imide **I1** dimers are only HBs. QTAIM shows no repulsion of either kind O_{HB}...O_{HB}, H...H or O_{HB}...O_S. In particular, we did not detect either attractive or repulsive interactions involving the spectator carbonyl moieties in the analysed imide dimers (Table S1 in the ESI† shows the QTAIM results for the complete set of investigated systems). Nevertheless, QTAIM can be too restrictive in the identification of relevant non-covalent interactions, as it is the case of the weak HB in ethylene glycol.⁴⁰ Therefore, we decided to use the IQA energy partition to determine the attractive or repulsive character of the intermolecular interactions that involve the spectator carbonyls in imide dimers. The left part of Table 4 shows the IQA interaction energies of a spectator oxygen (O13 in the **I1** molecule displayed in green) with the atoms of another **I1** monomer (shown in orange). We



Table 3 Amides and imides examined in this work. The dimerisation constants, K_{dimer} , were measured in CDCl_3 at 25 °C. The reported $\text{p}K_{\text{a}}$ values in DMSO and H_2O are shown in square brackets and parentheses respectively

Key	Structure	K_{dimer}^a (M^{-1})	$\text{p}K_{\text{a}}$	Key	Structure	K_{dimer}^a (M^{-1})	$\text{p}K_{\text{a}}$	Key	Structure	K_{dimer}^a (M^{-1})	$\text{p}K_{\text{a}}$
A1		2.7	[24.2] ²⁴	I1		1.4, K_{corr} : 0.4 ^b	(11.4) ^{c,25}	I8		8.6	(9.0) ^{d,26}
A2		8.3	[20.8] ²⁷	I2		3.3, K_{corr} : 0.8 ^b	[14.7] ^{c,33} (9.6) ^{c,28}	I9		12.7 (ref. 29)	(9.3) ^{d,29}
A3		1.0 (ref. 30)		I3		2.1, K_{corr} : 0.5 ^b	[13.4] ^{c,31} (10.2) ^{c,32}	I10		3.1 (ref. 29)	(8.2) ^{d,29}
A4		740.0	[17.0] ³³ (11.7) ³⁴	I4		1.2, K_{corr} : 0.3 ^b	(4.4) ³⁵	I11		5.3 (ref. 29)	(8.7) ^{d,29}
A5		1.8	[26.6] ²⁴	I5		2.6	(9.7) ^{e,36}	I12		8.0 (ref. 37)	(9.0) ^{d,26}
A6		8.0	[18.5] ²⁷	I6		4.1 (ref. 8)		I13		5.0 (ref. 37)	(7.9) ^{d,38}
A7		7.6		I7		2.7 (ref. 8)	(8.4) ^{e,39}				

^a The values of K_{dimer} were determined with errors lower than 2% (see Fig. S2–S13 in the ESI). ^b Statistical factor applied to imides with equivalent (or nearly equivalent) carbonyls and value of the corresponding corrected self-association constant (K_{corr}). ^c $\text{p}K_{\text{a}}$ of the compound without alkyl substituents. ^d $\text{p}K_{\text{a}}$ of the species without alcohol protecting groups. ^e Data for molecules with a methyl instead of a cyclohexyl substituent.



note that the interaction between O_{HB} and O_S is indeed strongly repulsive (pair $O13 \cdots O25$ in Table 4) because of the electrostatic repulsion between oxygens in accordance with the JSIH. The same atom O_S presents however other pairwise interactions which contribute to the attraction between the two monomers (e.g., pairs $O13 \cdots C14$ and $O13 \cdots C15$). After considering all the atoms of the neighbouring molecule, the atom O_S has an overall repulsion with the interacting monomer ($+10.7 \text{ kcal mol}^{-1}$). The nearly parallel $C=O_{HB}$ and $C=O_S$ dipoles also present a slight repulsive interaction between them ($1.1 \text{ kcal mol}^{-1}$ in each case).

The same analysis can also be carried out for every atom in one monomer (say those displayed in green in Table 4, with the corresponding results shown in the right of the same chart) to obtain the complete IQA interaction energy of the system. The results indicate that not only the atoms considered in the JSIH contribute significantly to the formation of the molecular cluster. In particular, the carbon of the spectator carbonyl group (C1) shows an attraction to the adjacent molecule. The attractive interaction of C1 towards the contiguous monomer more than compensates the repulsion of O13 ($-12.5 \text{ kcal mol}^{-1} + 10.7 \text{ kcal mol}^{-1} = -1.8 \text{ kcal mol}^{-1}$). We computed the same value for the other spectator carbonyl group. This attraction between the spectator carbonyl moiety and the whole interacting molecule evidences the numerous relevant intermolecular atomic pairwise interactions in the system.

The importance of the intermolecular interactions not considered by the JSIH in hydrogen-bonded dimers had already been pointed out by Popelier and Joubert.⁴¹ Their results were not in accordance with the JSIH in a detailed examination of the

relative energetic stability of 27 naturally occurring H-bonded nitrogen base pairs in the gas phase. These researchers considered multipolar expansions of the electrostatic energy (i.e., charge–charge, charge–dipole *etc.* contacts) which included up to terms which depend on R^{-6} (e.g. dipole–hexadecapole and quadrupole–octupole interactions), R being the distance between two multipoles. One of the main conclusions of this study concerns the difficulty to explain the relative stability of H-bonded clusters by only considering a subset of atomic pairs located in the boundaries between the interacting monomers as opposed to taking into account the whole set of intermolecular pairs of atoms in the system.

(ii) **Disruption of the resonance-assisted hydrogen bonds in imide dimers.** QTAIM analyses allowed us to consider the potential disruption of the resonance-assisted hydrogen bonds in imide dimers by virtue of their spectator carbonyl groups (top of Fig. 3). The eventual hindrance of the RAHB in the imide adducts would be accompanied by changes in the QTAIM Delocalisation Indices (DIs)⁴² and the IQA exchange–correlation component of the C–N and C=O bonds as schematised in Fig. 1-ii. The DIs, which decrease because of self-association, describe interactions whose covalent character diminishes because of the intermolecular HBs. Conversely, a positive value for ΔDI evidences a chemical bond with an increased covalent character following the formation of the dimer. The same trend analysis can be applied to the change in the magnitude of the IQA exchange–correlation contribution $\Delta|V_{XC}|$ of these bonds. The results shown in the bottom of Fig. 3 indicate that there is no such disruption of the RAHB in imide dimers due to these spectator carbonyl groups. The lengths (Table S10 in the ESI†) along with the $\Delta|V_{XC}|$ values and the ΔDIs for the C–N and C=Os bonds are barely affected. Moreover, in most cases the ΔDI of the spectator C=O and the absolute value of V_{XC}

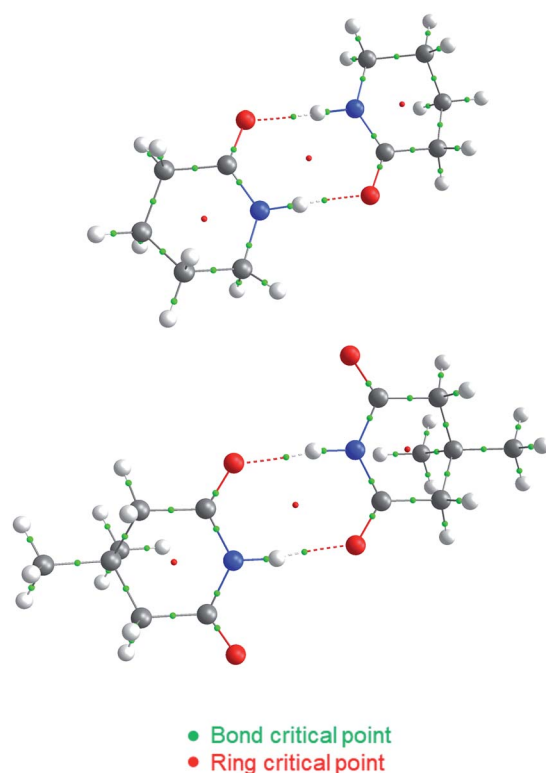


Fig. 2 QTAIM molecular graphs for dimers of A5 (top) and I1 (bottom). The bond and ring critical points are indicated.

Table 4 E_{int} (IQA) values with the largest magnitudes in homodimer I1-I1.^a The data are reported in kcal mol^{-1} . The full set of IQA interaction energies can be found in Table S3 in the ESI

O_s of I1	Atoms of I1	E_{int}	Atoms of I1	E_{int} (with all atoms of I1)
O13	C14	-79.2	C1	-12.5
	C15	-113.9	C2	4.0
	H23	-37.6	H10	-22.3
	N24	81.7	N11	5.1
	O25	114.0	O12	-30.9
	O26	60.6	O13	10.7
	Total	10.7	Total	-46.8

^a The IQA deformation energies of the interacting monomers are 16.4 and $20.0 \text{ kcal mol}^{-1}$, therefore the IQA formation energy of the molecular cluster is $E_{form} = (16.4 + 20.0 - 46.8) \text{ kcal mol}^{-1} = -10.4 \text{ kcal mol}^{-1}$.



increase slightly because of the formation of the RAHB in imide dimers as opposed to the flux of electrons suggested at the top of Fig. 3.

Additionally, the changes in the DIs and distances of the bonds involved in this RAHB are substantially larger than those of the neighbouring C–N and C=O interactions. These data point out that the disruption of the RAHB in imides is not the factor which explains the larger self-association of amides with respect to imides, a condition consistent with the observation that electron delocalisation is not the most stabilizing effect in resonance-assisted hydrogen bonds.⁴⁴

(iii) Intrinsic acid/base properties of amides and imides.

We test now the hypothesis that the differences for self-association between amides and imides are governed by the acidity of the amidic or imidic hydrogen and the basicity of the acceptor carbonyl group. For this purpose, we considered a model which is based on the energies associated with the N–H deprotonation, $E(A)$, and C=O protonation, $E(B)$, as shown in Fig. 4.⁴⁵ The acidity of the N–H proton is reduced with the magnitude of $|E(A)|$ while a high value of $|E(B)|$ indicates a strong basicity of the oxygen in the carbonyl group. The deprotonation energies for a wide variety of species which include imides, amides, (thio)ureas,⁴⁶ squaramides⁴⁷ and carboxylic acids⁴⁸ correlate very well with the corresponding experimental pK_a values, ditto for $|E(B)|$ and pK_{BH^+} , which indicates the pK_a of the conjugate acid of the species under consideration (see Tables S7, S8 and Fig. S29, S30 in the ESI† for the data of the complete set of compounds). Subsequently, we calculated $|E(A)|$ and $|E(B)|$ for compounds **A1–A7** and **I1–I13** (Table 5).

As expected, imides are more acidic and less basic than amides as suggested by the resonance structures in Fig. 1-iii.

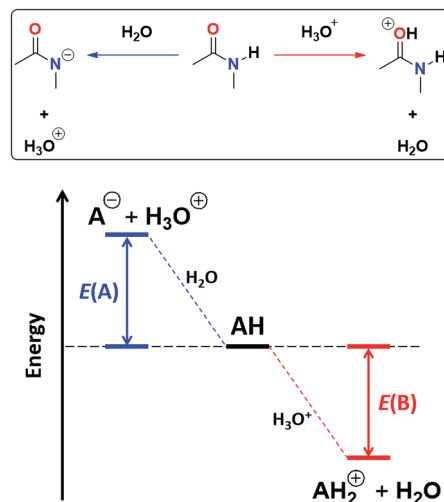


Fig. 4 Combined acidity and basicity model of the monomeric species to address the homocoupling of amides and imides. $|E(A)|$ and $|E(B)|$ are the respective magnitudes of the energies associated with the deprotonation and protonation reactions of the N–H and C=O fragments.

The change in Brønsted–Lowry acidity or basicity can substantially modify the self-association constants of hydrogen-bonded systems.^{21,52} We found a good correlation of $\ln K_{\text{dimer}}$ as a function of $|E(A)|$ and $|E(B)|$ whose distribution of points adjusts to a first-degree polynomial model. The species **A2** was not contemplated in the correlation because it is a cyclic carbamate that can form bifurcated hydrogen bonds with CHCl_3 as indicated by DFT geometry optimisations and schematised in

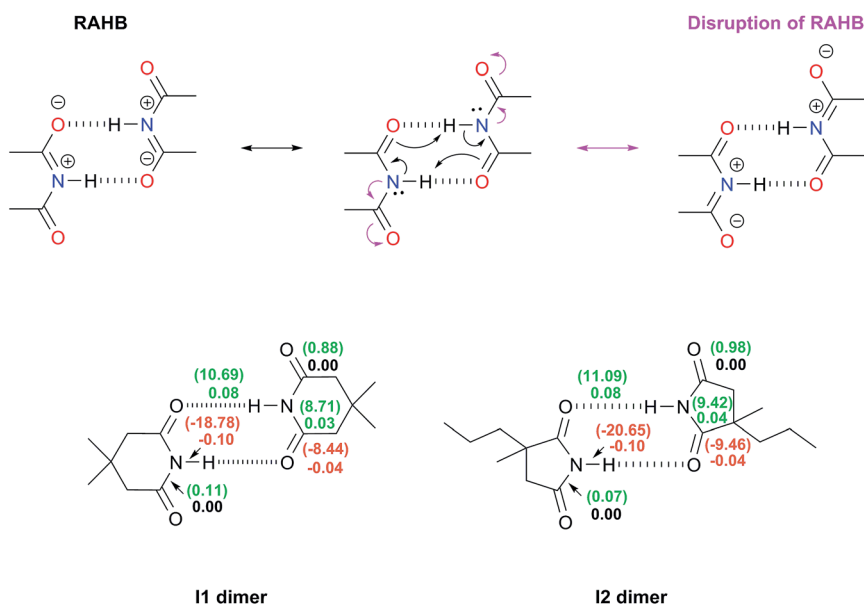


Fig. 3 Top: representation of the RAHB and its potential disruption (in magenta) within imide dimers by virtue of the electron-withdrawing nature of their spectator carbonyl groups. Bottom: changes in the electron delocalisation indices around the RAHBs as a consequence of the dimerisation of **I1** and **I2**. The positive values of $\Delta\text{DI} = \text{DI}(\text{in dimer}) - \text{DI}(\text{in monomer})$ are written in green while those which are negative are displayed in red. The corresponding change of the IQA exchange–correlation component, $\Delta|V_{\text{XC}}|/\text{kcal mol}^{-1}$, between two atoms is indicated in parentheses.



Table 5 $\ln K_{\text{dimer}}$ of the compounds shown in Table 3. The $|E(B)|$ and $|E(A)|$ values were computed with the SMD-(CHCl₃)-M06-2x/6-311++G(2d,2p) approximation

Compound	$ E(A) $ (kcal mol ⁻¹)	$ E(B) $ (kcal mol ⁻¹)	$\ln K_{\text{dimer}}$
A1	90.6	27.0	0.97
A2	84.5	17.6	2.11
A3	95.4	28.0	0.01
A4	78.1	28.8	6.61
A5	94.4	28.6	0.59
A6	79.7	19.6	2.07
A7	79.9	19.8	2.03
I1	80.3	13.9	-1.08 ^b
I2	75.4	12.9 ^a	-0.18 ^b
I3	73.8	10.8 ^a	-0.63 ^b
I4	73.6	7.7	-1.21 ^b
I5	82.5	20.8 ^a	0.96
I6	74.0	15.5	1.41
I7	74.9	13.7	0.99
I8	74.9	18.1 ^a	2.15
I9	77.8	22.8 ^a	2.54
I10	73.9	14.3 ^a	1.13
I11	72.4 ^c	11.9 ^c	1.67
I12	75.5	19.5 ^a	2.08
I13	71.7	15.3	1.61

^a $|E(B)|$ value of the most basic oxygen atom within the molecule.⁴³ (e.g. in **I5**, $|E(B)|$ for the other carbonyl group equals 16.1 kcal mol⁻¹).

^b $\ln K_{\text{dimer}}$ after the consideration of the statistical factor. ^c Data for the compound without methyl groups.

Fig. S31 in the ESI.† We conjectured that this feature can substantially affect the self-association of **A2** in comparison with the rest of the studied compounds. Indeed, the exclusion of **A2** improved the value of r^2 in Fig. 5 considerably. We note that the coefficients multiplying $|E(B)|$ and $|E(A)|$ ($C_{|E(B)|}$ and $C_{|E(A)|}$) are positive and negative respectively. These conditions support the model that self-association increases with the acidity of the N-H moiety and the basicity of the C=O group. Besides, $|C_{|E(B)|}| > |C_{|E(A)|}|$, and hence the dimerisation processes of the examined compounds are more sensitive to changes in the basicity of the carbonyl group than to modifications of the acidity of the amidic or imidic hydrogen. In general, this model points out that a high acidity or basicity by itself does not ensure a large association constant since there must be a balance between these properties to observe a substantial value of K_{dimer} . In other words, very poor acceptor or donor features of a system can substantially hinder its self-association process as it is the case for imides and basic amides **A3** and **A5** respectively. This analysis indicates that the low basicity of the carbonyl groups in imides allows us to explain why these compounds dimerise less strongly than amides notwithstanding their larger acidic character. The model in Fig. 5 allows us to interpret a series of experimental observations in CDCl₃. For example, the lowest value of the dimerisation constant corresponds to maleimide **I4**, a compound with high acidity but the one with the smallest basicity among the analysed systems. On the other hand, **A4** undergoes the strongest self-association among the molecules

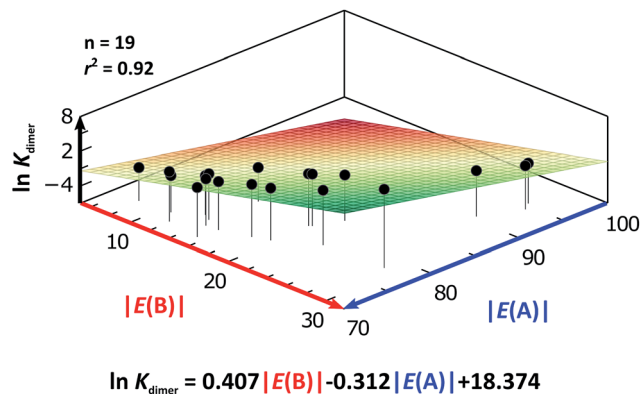


Fig. 5 $\ln K_{\text{dimer}}$ as a function of $|E(A)|$ and $|E(B)|$ (given in kcal mol⁻¹) for the compounds shown in Table 3 and the first-degree model adjusted for the distribution of points.

of interest. It has the highest basicity and an acidic character similar to the examined imides. These results point out that the occurrence of an aromatic sextet (top of Fig. 6) might favor zwitterionic structures that lead to a high self-association constant.⁴⁹ The relevance of the basicity of the C=O fragments in the self-association of amides and imides is also observed for the uracil analogues **I6–I13**. These imides are more basic than other compounds with the same functional group and hence dimerise more strongly. Furthermore, the consideration of the basicity of the C=O groups is also useful to rationalise which fragments are involved in the dimerisation. For example, it is well known that uracil derivatives (**I6**, **I8**, **I9**, **I12** and **I13**) form hydrogen bonds with the oxygen at C-4 rather than the one at C-2.²⁹ This finding is consistent with our results

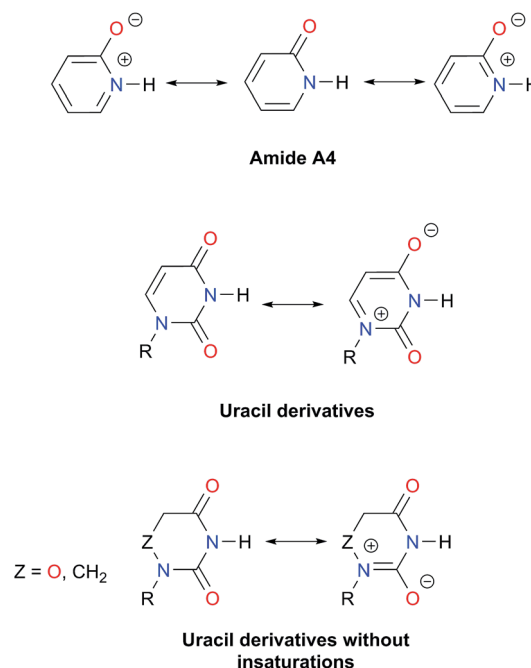


Fig. 6 Resonance structures of amide **A4**, uracil derivatives and their saturated analogues.



which indicate that the carbonyl at position four is more basic than its counterpart at position two. The larger basicity of the oxygen bonded to C-4 is associated with the condition that the corresponding carbonyl is conjugated with N-1 *via* a C-5, C-6 double bond. When this is no longer the case, *e.g.* **I5** and **I11**, the most basic carbonyl is the one at C-2 as illustrated in the middle and bottom of Fig. 6 (uracil derivatives with and without unsaturations). These observations are supported by the model proposed herein, 2D-NOE analyses²⁹ and proton affinity calculations for **I5** (Table 5).

Following the same arguments concerning the relative importance of basicity and acidity of the examined compounds, we can explain why among the studied five-membered heterocycles, amide **A1** associates more strongly than imides **I2** and **I4**. Six-membered rings also follow this trend, as observed when comparing **A4** *vs.* **I5–I13**. The same occurs with derivatives of benzene **A6**, **A7** *vs.* **I3** as shown in Fig. 7. On the other hand, when two species have a comparable acceptor capacity, the factor which establishes the stronger self-association is the N–H acidity. In this way, we can explain the differences in self-association between compounds of the same family, such as amides **A3**, **A5** and **A1** or imides **I2** *vs.* **I1**. Another appealing

feature of this model is that it explains the unexpected result that the uracil-containing species dimerise more strongly than amides **A5** or **A3**. Given that all these uracil derivatives have similar acidities, the dimerisation strength is, in this case, based on the variation of the C=O basicities. In addition, there is a good correlation between the experimental values of $\ln K_{\text{dimer}}$ with those predicted in the model of Fig. 5 as shown in Fig. S32 in the ESI.† Thus, the consideration of the proton acceptor and donor capacities described in this research is a reasonable alternative approach to interpret the differences in the self-association of amides and imides.

Self-association in CCl₄

We considered amide and imide dimerisation constants reported in CCl₄ as well.^{21,50} As discussed above, the apolar nature of carbon tetrachloride results in larger dimerisation constants than those obtained in CDCl₃ (ref. 51) (Fig. 8). The set of examined compounds comprises a variety of systems with electron donor and acceptor fragments and hence it allows us to consider the effect of these functional groups on $\ln K_{\text{dimer}}$. Similar to the previous discussion of the results in chloroform,

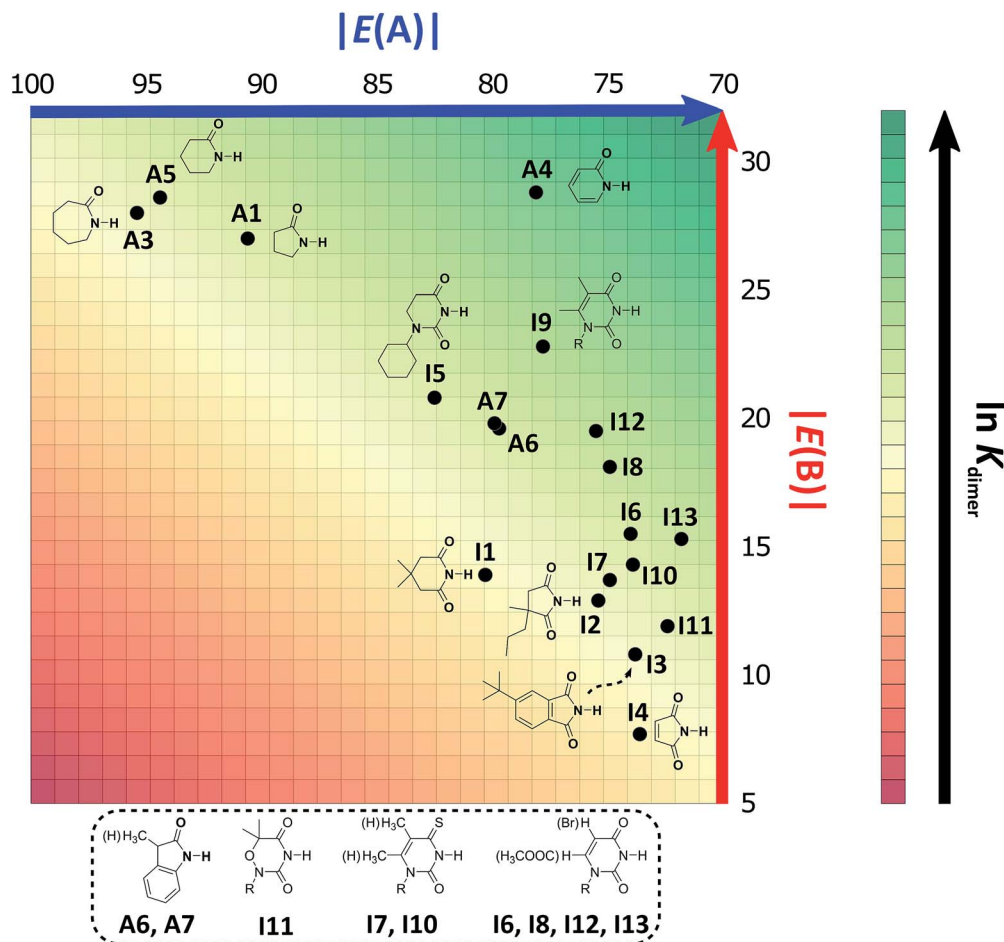


Fig. 7 2D graphical representation of the association strength of the investigated set of compounds in CDCl₃ as a function of acidity and basicity of the N–H and C=O groups respectively. The $|E(A)|$ and $|E(B)|$ values are displayed in kcal mol⁻¹. We indicate the structure and location of each species in the acid/base plane.



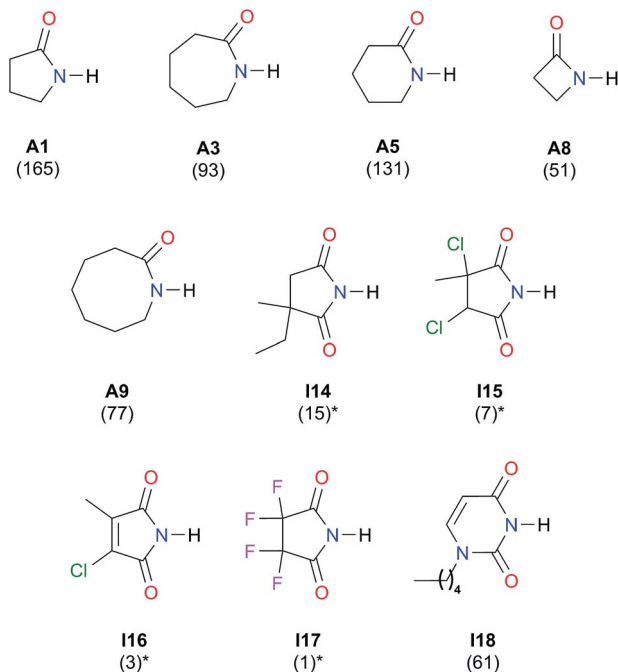


Fig. 8 Self-association constants (M^{-1}) reported in CCl_4 by IR spectroscopy.^{21,50} *The values were corrected by a statistical factor of four.

there is a correlation between (i) $\ln K_{dimer}$ and (ii) the basicity of the carbonyl group together with the acidity of the N-H moiety as shown in Fig. 9. The models of Fig. 5 and 9 are qualitatively similar. In particular, $C_{|E(B)|} > 0$, $C_{|E(A)|} < 0$ and $|C_{|E(B)|}| > |C_{|E(A)|}|$. The last-mentioned condition indicates once again that the dimerisation constant of amides and imides is more sensitive to the basicity of the carbonyl group than to the acidity of the N-H moiety, hence the larger association of amides in comparison to imides.

Analysis of heterodimers

The examination of heterodimers gives further insights about the dimerisation of amides and imides. The determination of K_{heter} indicates that hetero-association between **A5** and **I1** is stronger than in each homodimer as illustrated in Fig. 10. To rationalise this observation, we consider the relative strength of the individual HBs involved in the heterodimerisation and compared them with those in the homodimers. First, we took into account 1H -NMR spectroscopy results. The change in the N-H chemical shift due to complexation, $\Delta\delta_{N-H}$, is reported to increase with the strength of the association.^{52,53} The change in chemical shift of the imidic hydrogen within the **A5-I1** adduct (HB-1 in Fig. 10) is larger than that in the **A5** homodimer. Furthermore, the value of $\Delta\delta_{N-H}$ in the amidic hydrogen (HB-2 in the same figure) involved in the heterodimer is smaller than the corresponding value for the HB in the imide homodimer. Fig. S15† shows similar results obtained for **A1** and **I2** heterodimers. The measurement of K_{heter} was performed with a constant total amount of amide **A1** while imide **I2** was added to the system. The value of δ_{N-H} diminished through the titration, a condition indicative of a weakening of the HB entailing

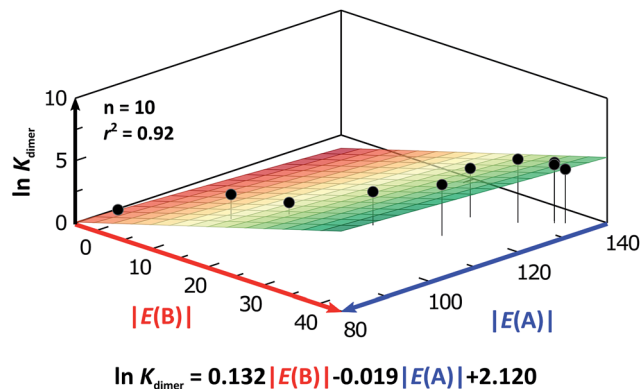
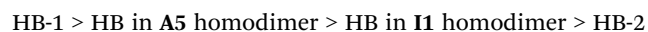


Fig. 9 $\ln K_{dimer}$ as a function of $|E(A)|$ and $|E(B)|$ (given in $kcal\ mol^{-1}$) of the molecules shown in Fig. 8 and studied in CCl_4 . The resulting first-degree model adjusted for the distribution of points is reported as well. The corresponding data are reported in Table S9 in the ESI.†

the amidic hydrogen. In the opposite experiment (having a constant total amount of **I2** and titrating with **A1**) the value of δ_{N-H} for the imidic proton increased more than in the corresponding homodimers, evidencing the strengthening of the hydrogen bond of the heterodimer which involves this proton. The last-mentioned effect is also observed in the **A5-I1** molecular cluster.

Concerning the **A5-I1** and **A1-I2** heterodimers, the strongest HB-1 is formed between the most acidic proton (the one in the imide) and the most basic carbonyl (found within the amide). On the other hand, the weakest HB takes place in the interaction of the less acidic proton, *i.e.* N-H of amides **A5** and the less basic carbonyl (the one in the imide). The strengths of the HBs in the amide and imide homodimers are between these two extremes. These results along with those of DFT geometry optimisations of the **A5-I1** heterodimer show the following trend of descending HB strength:



This order is similar to that found by Jorgensen¹⁰ and Leszczynski⁵⁴ who studied computationally the hetero- and homodimers of 2-pyrrolidone and succinimide. According to the JSIH, we should expect the hydrogen bond lengths within the heterodimer to be located somewhere between those of the homodimers. Moreover, the shortest hydrogen bond HB-1 is observed next to a presumed electrostatic or dipole-dipole repulsion involving the spectator carbonyl of **A5** as opposed to HB-2 which does not present this effect. Despite the aforementioned agreement of the JSIH with structural data, this hypothesis is not completely consistent with the H-bond strength and distance patterns found in the heterodimers. In contrast, the consideration of the acidity and the basicity of the N-H and C=O fragments explains the observed association constants, hydrogen bond distances and chemical shift patterns in these systems. The QTAIM and IQA analysis of the intermolecular interactions within the heterodimers **A5-I1** (Table 6) and **A1-I2** (Tables S5 and S6 in the ESI†) is consistent



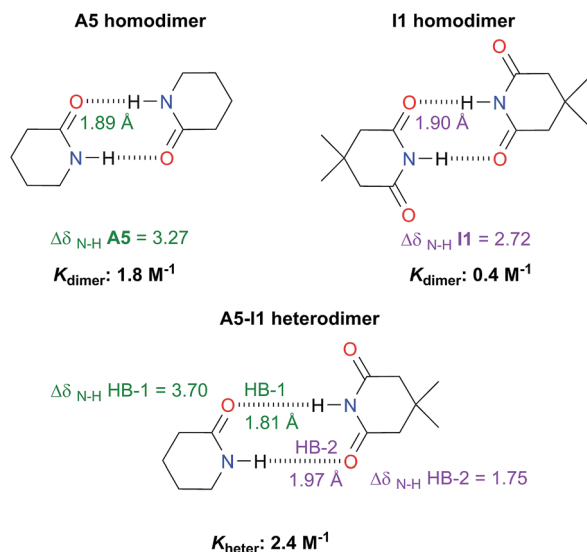


Fig. 10 Association constants (considering the statistical factor correction) and changes in chemical shift $\Delta\delta_{\text{N-H}}$ (in ppm) of the imidic and amidic protons within the **A5**, **I1**, hetero- and homodimers at infinite dilution (complete information in Fig. S14 in the ESI†). We also show the hydrogen bond lengths calculated at the SMD-(CHCl₃)-M06-2x/6-311++G(2d,2p) approximation.

with the previous discussion. The oxygen of the spectator C=O in the imide presents a strong repulsion with the oxygen of the neighbouring carbonyl involved in the HB and with the rest of the molecules of the amide. These repulsions are even stronger than in the case of the **I1** homodimer. Still, the hydrogen bond closest to the O_s atom in the **A5-I1** heterodimer is the strongest of the system. The relative strength of these HBs is revealed by their lengths as previously discussed and other indices used in the study of hydrogen bonds which include (i) Espinosa's empirical formula⁵⁵ (Fig. S28 in the ESI†) and (ii) the IQA intermolecular attractions with the interacting molecule (H10 along with O32 on one hand and H31 together with O12 on the other) as reported in the middle and right of Table 6. Despite the repulsion of the oxygen in the spectator carbonyl, this C=O group has an overall attractive interaction with the neighbouring imide or amide in a similar fashion to the corresponding homodimers. These IQA homo- and heterodimer results point out that the O_{HB}...O_s repulsions or those between the corresponding dipole carbonyls are not the decisive factor for the energetics of the amide and imide dimerisation.

Significance in the field of molecular recognition

Our investigation provides an alternative model to the JSIH to rationalise experimental observations concerning the homo- and heterodimerisation of amides and imides, for example, the hydrogen bond distance pattern in amide/imide heterodimers and the relative magnitude of K_{dimer} for these systems. The interplay of acidity and basicity allows us to explain other baffling results *e.g.* the fact that 2-ethyl-2-methylsuccinimide self-associates much more strongly (by a factor of 15) than tetrafluorosuccinimide.²¹ Based on the common consideration of

Table 6 E_{int} (IQA) values with the largest magnitudes within the **I1-A5** heterodimer. The data are reported in kcal mol⁻¹. The full set of IQA interaction energies can be found in Table S4 in the ESI†

O _s of I1	Atoms of A5	E_{int}	Atoms of I1	E_{int} (with all atoms of A5)	Atoms of A5	E_{int} (with all atoms of I1)
O13	C21	-23.2	C1	-19.9	C25	6.6
	C25	-118.4	H10	-32.9	H31	-19.7
	N26	83.1	O12	-28.6	O32	-40.7
	H31	-35.5	O13	16.9		
	O32	121.4				
Total		16.9	Total	-54.0	Total	-54.0

^a The IQA deformation energies of the amide and imide are 20.9 and 21.7 kcal mol⁻¹, so that the IQA formation energy of the molecular cluster is $E_{\text{form}} = (20.9 + 21.7 - 54.0) = -11.4$ kcal mol⁻¹.

the N-H acidity alone, it is expected that the last-mentioned compound would have a larger K_{dimer} . Likewise and according to the JSIH, the fluorinated compound should dimerise to a larger extent because the charges in the carbonyl oxygens are less negative than those in the alkylated succinimide. The alternative explanation that we offer is that the fluorine atoms reduce substantially the basicity of the carbonyls, thereby impairing the self-association of this compound.

Additionally, our results can be useful in understanding why amides are much more used in many technologies such as crystal engineering, development of materials and pharmaceuticals than imides.⁵⁶ The analysis presented herein indicates that self-association of these functional groups is more sensitive to the basicity of the C=O moiety than it is to the acidity of the N-H group. Hence, the modification of the basicity of this carbonyl represents a good opportunity in the modulation of the strength of the non-covalent interactions established by these groups. For example, the change of a carbonyl in a crucial amide for a more basic imino fragment in vancomycin enhances the association properties with the cell wall of bacteria immune to this antibiotic.⁵⁷ This increase of association restores antimicrobial activity and represents a strategy to address vancomycin-resistant infections.

Finally, the results of our investigation suggest a different approach for the analysis of the stability of multiple hydrogen-bonded systems such as uracil-diamino purine, cytosine-guanine and ADA-DAD systems.^{58,59} Generally, these systems are examined by considering only the acidity and basicity of the intermediate hydrogen bond and the JSIH. It would be nevertheless desirable to examine the Brønsted-Lowry acid/base properties for every HB in the system which could lead to valuable insights about the molecular recognition of hydrogen-bonded homo- and heterodimers.



Experimental

General experimental and computational details are given in the ESI.†

Conclusions

We investigated the reasons underlying the stronger self-association of amides as compared to imides. Our results indicate that the spectator carbonyl presents indeed repulsions with the oxygens involved in the HB but these repulsive interactions are not the key factor in the energetics of the H-bonded systems examined herein. This statement is based on the relevance of the pairwise interactions which are not accounted for by the JSIH and the experimental and theoretical examination of amide-imide homo- and heterodimers. Our results also reveal that the spectator carbonyl groups in imides do not interfere with the resonance-assisted hydrogen bonds in the dimers of these species. Then, we consider the Brønsted-Lowry acid/base properties of the HB donors and acceptors involved in the interaction within these molecular aggregates. The examination of the basicity of the C=O group, the acidity of the N-H moiety and K_{dimer} resulted in a first-degree model suggesting that the proton acceptor capacity of the carbonyl group is more important than the acidity of the amidic or imidic hydrogens for the self-association of the investigated compounds. This model also indicates that there must be a balance between the respective acidity and basicity of the N-H and C=O fragments to observe a substantial self-association of these systems. Particularly, amides exhibit larger self-association constants because of their higher basicities in comparison with imides. Similar conclusions were drawn from systems investigated in CCl_4 . Our results also explain the hydrogen bond distance patterns found in amide and imide homo- and heterodimers. The acidity/basicity balance in the dimerisation of amides and imides is an alternative approach to the JSIH in order to explain this phenomenon. Overall, we expect that the application of the insights presented herein will prove valuable to understand and modulate hydrogen bonds between the investigated functional groups which are present in a wide variety of supramolecular systems throughout biology and chemistry.

Conflicts of interest

There are no conflicts to declare.

Acknowledgements

The authors gratefully acknowledge computer time from DGTIC/UNAM (projects LANCAD-UNAM-DGTIC-250 and 252), financial support from DGAPA-UNAM (grant IN207318), CONACyT/México (grants 254014 and 253776) and the Ph.D. scholarships No. 273438 and 336875 to W. E. V. N and E. I. J respectively. This study benefits from resources at LURMN in IQ-UNAM, financed by CONACYT Mexico (Project: 0224747) and UNAM. We are indebted to Prof. Anatoli Iatsimirski for performing the calculations of the heterodimerisation constants

and for his important contributions to this work. We also thank M. Sc. E. Hernández-Huerta for support in the search for information from the literature and Dr V. Duarte-Alaniz for his assistance on data graphing. In addition, we are grateful to F. J. Pérez, L. Velasco, and M. C. García for mass analysis, and M. A. Peña, E. Huerta, H. Ríos and R. Gaviño for recording NMR experiments, as well as M. Aguilar-Araiza, D. Vázquez-Cuevas and G. Cortés-Romero for technical support.

Notes and references

- 1 L. Pauling, R. B. Corey and H. R. Branson, *Proc. Natl. Acad. Sci. U. S. A.*, 1951, **37**, 205–211.
- 2 A. E. García and K. Y. Sanbonmatsu, *Proc. Natl. Acad. Sci. U. S. A.*, 2002, **99**, 2782–2787.
- 3 R. Dahm, *Hum. Genet.*, 2008, **122**, 565–581.
- 4 (a) E. T. Kool, *Annu. Rev. Biophys. Biomol. Struct.*, 2001, **30**, 1–22; (b) K. M. Guckian, B. A. Schweitzer, R. X.-F. Ren, C. J. Sheils, D. C. Tahmassebi and E. T. Kool, *J. Am. Chem. Soc.*, 2000, **122**, 2213–2222.
- 5 (a) A. Diez-Martinez, E. K. Kim and R. Krishnamurthy, *J. Org. Chem.*, 2015, **80**, 7066–7075; (b) W. Jiang, K. Tiefenbacher, D. Ajami and J. Rebek, *Chem. Sci.*, 2012, **3**, 3022–3025.
- 6 (a) J. R. Quinn and S. C. Zimmerman, *Org. Lett.*, 2004, **6**, 1649–1652; (b) B. Askew, P. Ballester, C. Buhr, K. S. Jeong, S. Jones, K. Parris, K. Williams and J. Rebek, *J. Am. Chem. Soc.*, 1989, **111**, 1082–1090; (c) E. I. Jiménez, W. E. Vallejo Narváez, C. A. Román-Chavarría, J. Vazquez-Chavez, T. Rocha-Rinza and M. Hernández-Rodríguez, *J. Org. Chem.*, 2016, **81**, 7419–7431.
- 7 (a) J. M. Purcell, H. Susi and J. R. Cavanaugh, *Can. J. Chem.*, 1969, **47**, 3655–3660; (b) W. Luo, C. Lin, J. Lin, Dah-YuKao and J. Chen, *J. Chin. Chem. Soc.*, 2000, **47**, 1177–1183.
- 8 (a) Y. Kyogoku, R. C. Lord and A. Rich, *Proc. Natl. Acad. Sci. U. S. A.*, 1967, **57**, 250–257; (b) T. Hupp, C. Sturm, E. M. Basilio Janke, M. P. Cabre, K. Weisz and B. Engels, *J. Phys. Chem. A*, 2005, **109**, 1703–1712.
- 9 K. S. Jeong, T. Tjivikua and J. Rebek, *J. Am. Chem. Soc.*, 1990, **112**, 3215–3217.
- 10 W. L. Jorgensen and D. L. Severance, *J. Am. Chem. Soc.*, 1991, **113**, 209–216.
- 11 W. L. Jorgensen and J. Pranata, *J. Am. Chem. Soc.*, 1990, **112**, 2008–2010.
- 12 (a) P. J. Cox and S. F. Parker, *Acta Crystallogr., Sect. C: Cryst. Struct. Commun.*, 1996, **52**, 2578–2580; (b) S. Hachiya, Y. Kasashima, F. Yagishita, T. Mino, H. Masu and M. Sakamoto, *Chem. Commun.*, 2013, **49**, 4776–4778; (c) M. Puszyńska-Tuszkano, M. Daszkiewicz, G. Maciejewska, Z. Staszak, J. Wietrzyk, B. Filip and M. Cieślak-Golonka, *Polyhedron*, 2011, **30**, 2016–2025.
- 13 R. R. Gardner and S. H. Gellman, *J. Am. Chem. Soc.*, 1995, **117**, 10411–10412.
- 14 J. R. Quinn, S. C. Zimmerman, J. E. Del Bene and I. Shavitt, *J. Am. Chem. Soc.*, 2007, **129**, 934–941.
- 15 T. J. Murray and S. C. Zimmerman, *J. Am. Chem. Soc.*, 1992, **114**, 4010–4011.
- 16 D. Rusinska-Roszak, *J. Phys. Chem. A*, 2015, **119**, 3674–3687.



- 17 J. Ho, C. J. Easton and M. L. Coote, *J. Am. Chem. Soc.*, 2010, **132**, 5515–5521.
- 18 R. F. W. Bader, *Atoms in Molecules; A quantum theory*, 1994.
- 19 M. A. Blanco, A. Martín Pendás and E. Francisco, *J. Chem. Theory Comput.*, 2005, **1**, 1096–1109.
- 20 A. E. Shchavlev, A. N. Pankratov, V. B. Borodulin and O. A. Chaplygina, *J. Phys. Chem. A*, 2005, **109**, 10982–10996.
- 21 J. Hine, S. Hahn and J. Hwang, *J. Org. Chem.*, 1988, **53**, 884–887.
- 22 A. V. Galanti, *J. Appl. Polym. Sci.*, 1984, **29**, 1611–1616.
- 23 E. J. Cabrita and S. Berger, *Magn. Reson. Chem.*, 2001, **39**, S142–S148.
- 24 F. G. Bordwell and H. E. Fried, *J. Org. Chem.*, 1991, **56**, 4218–4223.
- 25 G. Schwarzenbach and K. Lutz, *Helv. Chim. Acta*, 1940, **23**, 1139–1146.
- 26 M. Aljahdali, A. A. El-Sherif, M. M. Shoukry and S. E. Mohamed, *J. Solution Chem.*, 2013, **42**, 1028–1050.
- 27 F. G. Bordwell, J. E. Bartmess and J. A. Hautala, *J. Org. Chem.*, 1978, **43**, 3095–3101.
- 28 H. F. Walton and A. A. Schilt, *J. Am. Chem. Soc.*, 1952, **74**, 4995–4996.
- 29 A. Dunger, H. H. Limbach and K. Weisz, *Chem.–Eur. J.*, 1998, **4**, 621–628.
- 30 J. Chen, *J. Chem. Soc., Faraday Trans.*, 1994, **90**, 717–720.
- 31 I. Koppel, J. Koppel, F. Degerbeck, L. Grehn and U. Ragnarsson, *J. Org. Chem.*, 1991, **56**, 7172–7174.
- 32 R. A. McClelland, N. E. Seaman, J. M. Duff and R. E. Branston, *Can. J. Chem.*, 1985, **63**, 121–128.
- 33 F. G. Bordwell, *Acc. Chem. Res.*, 1988, **21**, 456–463.
- 34 J. W. Bunting, A. Toth, C. K. M. Heo and R. G. Moors, *J. Am. Chem. Soc.*, 1990, **112**, 8878–8885.
- 35 J. Von Sonntag, W. Knolle, S. Naumov and R. Mehnert, *Chem.–Eur. J.*, 2002, **8**, 4199–4209.
- 36 H. S. Levene, P. A. Bass and L. W. Simms, *J. Biol. Chem.*, 1926, **70**, 229–241.
- 37 A. Diez-Martinez, E. K. Kim and R. Krishnamurthy, *J. Org. Chem.*, 2015, **80**, 7066–7075.
- 38 J. Jonas and J. Gut, *Collect. Czech. Chem. Commun.*, 1962, **27**, 716–723.
- 39 A. Psoda, Z. Kazimierzczuk and D. Shugar, *J. Am. Chem. Soc.*, 1974, **96**, 6832–6839.
- 40 J. R. Lane, J. Contreras-García, J.-P. Piquemal, B. J. Miller and H. G. Kjaergaard, *J. Chem. Theory Comput.*, 2013, **9**, 3263–3266.
- 41 P. L. A. Popelier and L. Joubert, *J. Am. Chem. Soc.*, 2002, **124**, 8725–8729.
- 42 (a) The delocalisation indices represent a measure of the degree of covalency of a given pairwise interaction in a molecule or molecular cluster according to ref. 18; (b) M. García-Revilla, P. L. A. Popelier, E. Francisco and Á. Martín Pendás, *J. Chem. Theory Comput.*, 2011, **7**, 1704–1711; (c) X. Fradera, M. A. Austen and R. F. W. Bader, *J. Phys. Chem. A*, 1999, **103**, 304–314.
- 43 The carbonyl in position 4 of uracil derivatives participates to a greater extent in H-bonding than that in position 2, as shown by NMR experiments (ref. 29). The same reference also shows that for **I10** and **I11**, the C=O in position 2 participates more in the self-association than that in position 4. The proton affinity calculations of **I5** show that the most basic carbonyl for this compound is in position 2 (see Table 5).
- 44 J. M. Guevara-Vela, E. Romero-Montalvo, A. Costales, Á. M. Pendás and T. Rocha-Rinza, *Phys. Chem. Chem. Phys.*, 2016, **18**, 26383–26390.
- 45 Z. B. Maksić, B. Kovačević and R. Vianello, *Chem. Rev.*, 2012, **112**, 5240–5270.
- 46 G. Jakab, C. Tancon, Z. Zhang, K. M. Lippert and P. R. Schreiner, *Org. Lett.*, 2012, **14**, 1724–1727.
- 47 X. Ni, X. Li, Z. Wang and J. P. Cheng, *Org. Lett.*, 2014, **16**, 1786–1789.
- 48 F. G. Bordwell and D. Algrim, *J. Org. Chem.*, 1976, **41**, 2507–2508.
- 49 J. I. Wu, J. E. Jackson and P. V. R. Schleyer, *J. Am. Chem. Soc.*, 2014, **136**, 13526–13529.
- 50 N. A. Prokopenko, I. A. Bethea, C. J. Clemens IV, A. Klimek, K. Wargo, C. Spivey, K. Waziri and A. Grushow, *Phys. Chem. Chem. Phys.*, 2002, **4**, 490–495.
- 51 D. M. Porter and W. S. Brey, *J. Phys. Chem.*, 1967, **71**, 3779–3783.
- 52 T. Steiner, *Angew. Chem., Int. Ed.*, 2002, **41**, 48–76.
- 53 For example, amide **A4**, has the highest value of $\Delta\delta_{\text{N-H}}$ (5.69 ppm) and of the self-association constant as well (Table 3). The same trend can be observed for **A5** and **I1** (Fig. 10) and another structurally-related amide-imides pairs (Fig. S2 and S13 in the ESI†).
- 54 O. Lukin and J. Leszczynski, *J. Phys. Chem. A*, 2002, **106**, 6775–6782.
- 55 E. Espinosa, E. Molins and C. Lecomte, *Chem. Phys. Lett.*, 1998, **285**, 170–173.
- 56 N. Qiao, M. Li, W. Schlindwein, N. Malek, A. Davies and G. Trappitt, *Int. J. Pharm.*, 2011, **419**, 1–11.
- 57 J. Xie, J. G. Pierce, R. C. James, A. Okano and D. L. Boger, *J. Am. Chem. Soc.*, 2011, **133**, 13946–13949.
- 58 B. A. Blight, C. A. Hunter, D. A. Leigh, H. McNab and P. I. T. Thomson, *Nat. Chem.*, 2011, **3**, 244–248.
- 59 M. K. Tiwari and K. Vanka, *Chem. Sci.*, 2017, **8**, 1378–1390.

